Journal Pre-proof

Tectonic rotations in central Chile: New insights on the southern limit of the Maipo Orocline

C. Puigdomenech, S. Alarcón, V. Ruiz González, P. Rossel, D. Orts, C. Zaffarana

PII: S0895-9811(20)30555-1

DOI: https://doi.org/10.1016/j.jsames.2020.103012

Reference: SAMES 103012

To appear in: *Journal of South American Earth Sciences*

Received Date: 3 July 2020

Revised Date: 2 November 2020

Accepted Date: 4 November 2020

Please cite this article as: Puigdomenech, C., Alarcón, S., Ruiz González, V., Rossel, P., Orts, D., Zaffarana, C., Tectonic rotations in central Chile: New insights on the southern limit of the Maipo Orocline, *Journal of South American Earth Sciences* (2020), doi: https://doi.org/10.1016/j.jsames.2020.103012.

All persons who meet **authorship** criteria are listed as **authors**, and all **authors** certify that they have participated sufficiently in the work to take public responsibility for the content, including participation in the concept, design, analysis, writing, or revision of the manuscript.

Tectonic rotations in Central Chile: new insights on the southern limit of the Maipo Orocline

Puigdomenech, C. [(1)] *; Alarcón S. [(2)]; Ruiz González V. [(1)]; Rossel, P. [(2)]; Orts, D.[(34)]; Zaffarana C.[(34)]

[(1)] *IGEBA-CONICET* .
[(2)] *Universidad Andres Bello, Facultad de Ingeniería, Geología, Autopista Talcahuano, 7100 Concepción, Chile*
[(3)] *Consejo Nacional de Investigaciones Científicas y Técnicas (CONICET). Instituto de Investigación en Paleobiología y Geología. Río Negro, Argentina.*
[(4)] *Universidad Nacional de Río Negro. Instituto de Investigación en Paleobiología y Geología. Río Negro, Argentina.*

* Corresponding auhtor at: Departamento de Ciencias Geológicas, Pabellón 2, Ciudad Universitaria, Buenos Aires, C1428EHA, Argentina. E-mail address: carlapuigdo@gmail.com (C. Puigdomenech)

Abstract

The Maipo Transition Zone or Maipo Orocline represents a change in strike of the topography from N-S between 30º and 33ºS to an NNE-SSW trend to the south. The southern flank of the Maipo Orocline can be traced along strike to around 38ºS. There the Andean margin exposes another orogen bending, the Arauco Orocline. Although the tectonic evolution of this segment of the Andean chain is relatively well constrained, the limit between both oroclines is unclear. In this paper, we show the results of a paleomagnetic study carried out in three plutons of Upper Triassic age located along the Coastal Cordillera of central Chile between 35° to 37°S. Paleomagnetic analysis from Constitución Granite and Cobquecura Pluton shows an increase of clockwise vertical-axis rotations from north to south consistent with previous data, whereas results obtained in the Hualpén Stock, located to the south, shows minors counter-clockwise rotations. This change in the rotation pattern would reflect the Maipo and Arauco Oroclines limit. The similar amounts of tectonic rotations recorded by Mesozoic and Miocene rocks indicate that the whole area behaved as a single block and constrains the maximum possible age for the occurrence of tectonic rotations to Miocene.

Keywords: Maipo Orocline, Paleomagnetism, Tectonic rotation, Triassic Plutons

1. Introduction

The Andean Cordillera extends for more than 8000 km on South America's western margin from the Caribbean Sea at its north end to the Scotia Ridge at the south end. Although this mountain range is a continuous element, its geological history involves a complex record

of accretions, collisions and two important periods of subduction-related magmatism, the Carboniferous to Permian Gondwana Orogeny (e.g., Mpodozis and Ramos 1989; Bahlburg and Hervé 1997) and the Jurassic to Recent Andean Cycle, with its ongoing subduction along the Andean trench (e.g., Coira et al. 1982; Mpodozis and Ramos 1989). This generates a complicated segmentation where tectonics, magmatism and sedimentation processes change over time and space.

Three large pronounced curvatures of tectonic trends are present along the topographic front of the southern Central Andes, including important changes in the rotations pattern and from north to south these are the Vallenar, Maipo and Arauco oroclines (Arriagada et al. 2009, 2013; Ferrando et al. 2014).

The orocline concept was formulated by Carey (1955) for an orogenic system which has been flexed in plan view to an elbow shape in a subsequent deformation phase. While having a genetic connotation, this term is often incorrectly used in the literature as a geometric description for any orogenic curvature regardless of the actual kinematics of the curvature formation. One of the mechanisms most common involved in the formation of an orocline, proposed by Isacks (1988), is the presences of differential shortening along the belt causing tectonic rotations.

The Maipo Transition Zone (Yáñez et al. 2002) or Maipo Orocline (Farías et al. 2008) represents a change in strike in the topography, geologic units and major structures. The trend of major structures changes from N-S between 30º and 33ºS in the north to a NNE-SSW trend to the south. While the northern segment of the curvature corresponds with the ongoing subduction of the Pampean flat-slab segment, which converges nearly horizontally beneath the South American lithosphere, the southern segment coincides with the normal subduction segment developed to the south of 33ºS (Isacks 1988; Ramos et al. 2002).

Previous paleomagnetic analysis from Jurassic to Late Cretaceous rocks in the Chilean-Pampean flat-slab segment shows small to non-significant clockwise vertical-axis rotations (Beck et al. 1986, 1990; Creixell et al. 2006). In contrast, towards the south on the normal subduction segment, paleomagnetic results obtained in Late Jurassic to Neogene rocks show systematical clockwise rotations of up to 40º (Arriagada et al. 2013). The southern flank of the Maipo Orocline can be traced along strike to around 38ºS. There, the Andean margin exposes another orogen bending, the Arauco “Orocline” (Fig 1; Melnick et al. 2009).

However, currently, no detailed paleomagnetic studies confirm the occurrence of tectonic rotations and the limit between both oroclines is still unknown.

In Triassic to Jurassic times, the Chilean active continental margin experienced significant changes in the tectonic and magmatic regimes due to the transition from the Gondwana to the Andean subduction process. In the segment between 34° and 42°S, the Late Paleozoic-Early Mesozoic magmatic activity is typical for a magmatic arc experiencing abundant crustal recycling, with the formation of large granitic batholiths and decreasing magma volumes with time toward the Late Triassic (Martin et al. 1999; Lucassen et al. 2004). Early Mesozoic intrusions in the western part of the Cordillera de la Costa comprise, from north to south, La Estrella Granite, Pichilemu Granite, Constitución Granite, Cobquecura Pluton, and the Hualpén Stock. In this contribution, we report new paleomagnetic data of the Late Triassic Constitución, Cobquecura and Hualpen plutons, which crop out along the Cordillera de la Costa between 33 ° - 37 ° S. They are post-orogenic intrusions with respect to the Gondwanic orogenic cycle and their study allows us not only to investigate the southern limit of the Maipo Orocline but also to work out the possibility of tectonic rotations related to the Gondwana Breakup.

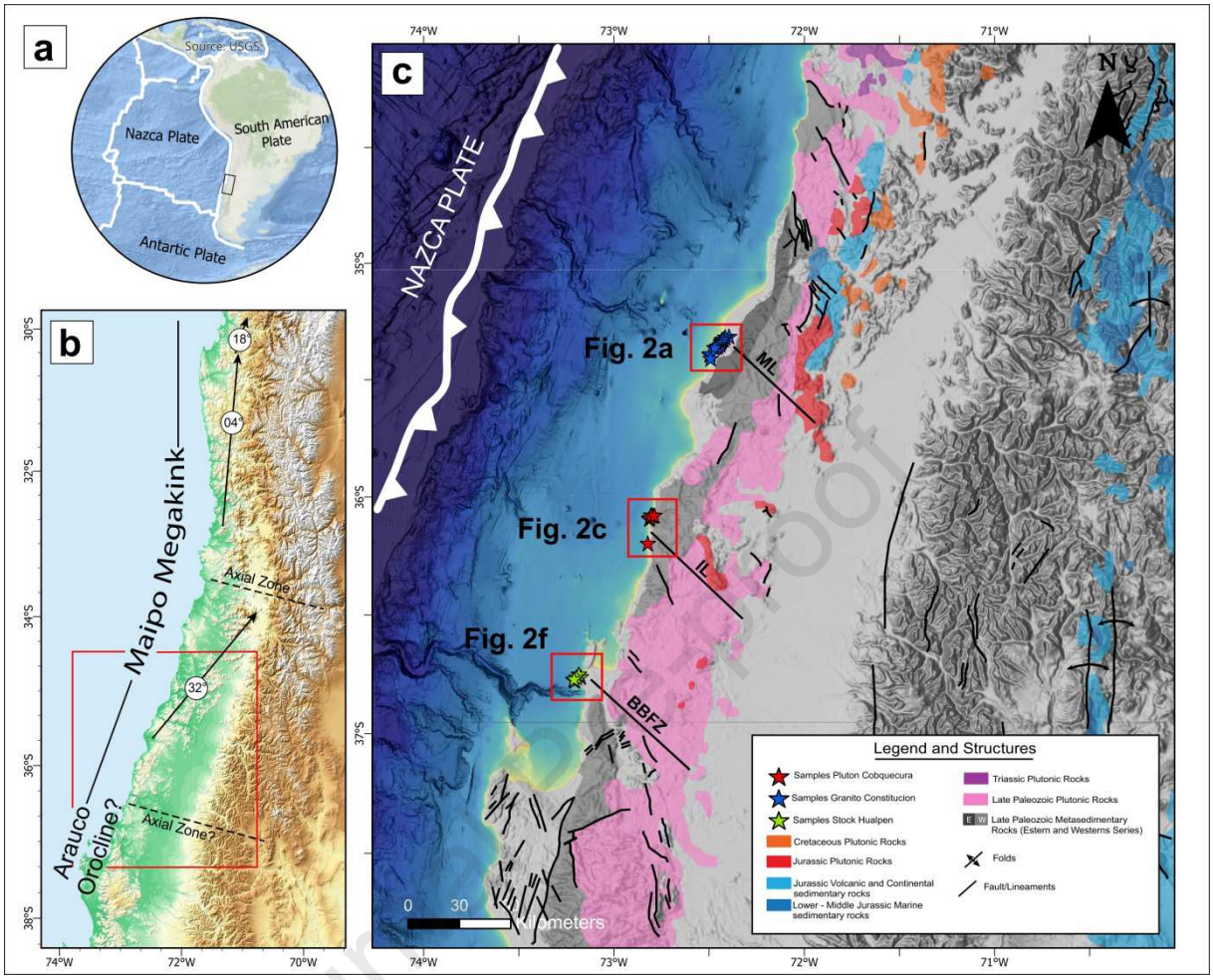

Figure 1: (A) Tectonics plates; the black box shows the study area. (B) Paleomagnetic rotations domains showing the Maipo and Arauco Oroclines (Arriagada et al 2009). (C) Geological map, the red boxes indicates the sampling areas. BBFZ: Bio-Bio Fault Zone(Rehak et al. 2008)**; ML: Maule Lineament and IL: Itata Lineament (Willner et al. 2005).**

2. Geological Setting

During the transit from the Gondwanan to the Andean subduction, the active continental margin experienced significant changes in the tectonic and magmatic regimes. The igneous activity in the Late Paleozoic between 34° and 42°S shows typical features of magmatic arc with abundant crustal recycling, with the formation of large granitic batholiths (Berg and Breitkreuz 1983; Berg et al. 1983), that intrude previously metamorphosed sedimentary units, leading to the formation of the Late Paleozoic Paired Metamorphic belt of Central and Southern Chile (Aguirre et al. 1972; Hervé et al. 1988).

The units that form this paired metamorphic complex are subdivided in the Western and the Eastern Series (Aguirre et al., 1972 and Fig. 1C). The Eastern Series consists of meta-greywacke and metapelite and is almost devoid of metabasites. It shows metamorphic

gradients from very low-grade rocks to amphibolite – granulite gneisses, related to the proximity of Late Paleozoic calcalkaline granitoids (Hervé et al. 1988; Beck et al. 1991; Martin et al. 1999). Based on petrological, structural, and age characteristics, the Eastern Series is interpreted as resulting from subduction-related accretion and deformation of former passive margin sediments, followed by intrusion of arc granitoids (Hervé et al. 1988; Willner et al. 2005; Glodny et al. 2006). The Western Series represents the accretionary prism and is characterized by meta-greywackes interlayered with lenses of oceanic crust. The latter consist of mainly green-schist, rare blue-schist and associated Fe-Mn-rich meta-sediments, minor meta-chert and serpentinite. All these rocks are pervasively deformed and characterized by a second flat-lying transposition foliation. The Western Series is interpreted as a paleoaccretionary complex built by basal accretion and the Eastern Series shows all characteristics of frontally accreted sediments (Glodny et al. 2005; Richter et al. 2007).

Subsequently, after the definitive amalgamation of Pangea Supercontinent in late Permian, the previously formed Orogen collapsed as result of the drastic diminish in plate convergence, leading to the formation of elongated NNW-SSE extensional basins and large volumes of mostly anorogenic silic magmatism of the Choiyoi province (Uliana and Biddle 1988; Mpodozis and Ramos 1989; Mpodozis and Kay 1990; Suarez and Bell 1992)

First evidence of post Gondwana magmatism in Southern Central Chile is a series of isolated Upper Triassic high silica granitoids that crops out in Coastal Cordillera (Vasquez et al., 2011). Their compositions are mainly monzogranitic (Hervé et al. 1988), except for the Cobquecura Pluton, which also comprises gabbroic rocks (Hervé et al. 1988; Vásquez et al. 2009). These plutonic rocks crop out on both the western and the eastern flanks of the Cordillera de la Costa (Hervé et al. 1988; Vásquez and Franz 2008). This granitoid intrudes exclusively Late Paleozoic magmatic and metamorphic rocks of the previous tectonic cycle, and are closely associated with small Upper Triassic sedimentary basins with an incipient northwest orientation (Charrier 1979; Hervé et al. 1988).

The Early Mesozoic Constitución, Cobquecura and Hualpén plutons were all emplaced at shallow crustal levels, display narrow contact aureoles, lack indications for deformation or metamorphism, are post-kinematic with respect to the main foliation of their metamorphic host rocks, and are exposed discontinuously in only small areas (Vásquez et al. 2011). The coincidence of the Triassic plutonic bodies with NW–SE trending lineaments have led Vázquez et al. (2011) to propose oblique subduction conditions generating extension-related NW–SE structures, which in turn facilitated the ascent of magmas followed by an

episode of slab steepening at around 210–197 Ma (Fig. 1C). Extensional conditions was maintained for most of Jurassic and Early Cretaceous time, permitting the dominance of extensional tectonic conditions on the continental margin, intense magmatic activity along the arc, and abundant sedimentation in the backarc basin. These basins were inverted during the Late Cretaceous compressive deformation and created a major regional unconformity (Charrier et al. 2009).

The Constitución Granite (35.36°S, 72.42°W; Fig. 2a and b) is a homogeneous, K-feldspar-porphyric biotite-monzogranite (Vásquez et al. 2011). It is intruded into metapelites and metabasites of the Late Paleozoic metamorphic basement. The Constitución Granite has been dated as 208 ±6 Ma; 202 ± 6 Ma by K-Ar in biotite by Gana and Hervé (1983). Older ages of 224 ± 1 Ma were obtained using Pb evaporation on zircon by Willner et al. (2005).

The Cobquecura Pluton is located to the south of Constitución Granite (~ 36°10'S, 72°47'W; Fig. 2c and d), intruded into the meta-sedimentary metamorphic basement. The pluton, compared with other intrusions of the area, shows a bi-modal composition with gabbroic and granitic end-members, and less abundant hybrid rocks consisting of tonalites evidencing mixing (resorbed cores of plagioclase) and mingling (composite dikes, mafic pillow-shaped enclaves and net-vein complexes) processes. This rock additionally contains a few metamorphic enclaves (Vásquez and Franz 2008). Abundant pillows of mafic composition in granitic magmas are typical for the mingling of coeval felsic and mafic magmas (Fig. 2d). Granites contain fayalitic olivine, Fe-rich clinopyroxene, amphibole, biotite, and ilmenite, whereas gabbros are mostly composed of Mg-rich piroxenes, amphiboles and minor forsteritic olivine and biotite (Vásquez et al. 2011). The age of the Cobquecura magmatism is fairly well constrained. A K–Ar age of 211±4 Ma on ferroedenitic amphibole was obtained for a fayalite granodiorite, a K–Ar Mg-hornblende age of 213±5 Ma for a gabbro (Vásquez et al. 2005) and 209 ± 2 Ma; 203 ± 2 Ma (sample 04-22) by U-Pb zircon (Vásquez et al. 2011). Field observations, namely the evidence for magma mingling, show that the mafic and felsic magmas of the Cobquecura Pluton were strictly contemporaneous. This inference is backed up by major element correlations for fayalite granitoids and gabbro, suggesting a co-magmatic evolution for all Cobquecura igneous rocks (Vásquez and Franz 2008).

The Hualpén Stock is located at the mouth of the Biobío River, which follows a NW–SE-oriented lineament. It intruded into metapelites of the Paleozoic metamorphic basement and is a homogeneous two mica–monzogranite (Fig. 2 f and g; Creixell et al. 2002). There are

precise geochronologic data for the stock (215 ± 4 Ma, K-Ar in biotite from Hervé et al. 1988; meanwhile an age by Rb-Sr mineral data 220±5 – 222±2 Ma has been mentioned by Lucassen et al. 2004, and 227 ± 7 Ma in Rb-Sr mineral data from Glodny et al. 2006).

3. Sampling and methodology

Paleomagnetic sampling was performed during two field seasons when more than 120 oriented cores were collected. The sampling was carried out with a portable gasoline-powered drill system, and all samples were oriented in situ using magnetic and solar compasses. The collection of oriented cores belongs to 23 stations and at least five different samples were obtained from each sampling site.

Magnetic remanences were measured with a JR6 spinner magnetometer in the Paleomagnetism Laboratory "Daniel A. Valencio" of the IGeBA (UBA-CONICET) and with the "SushiBar" magnetometer (a fully automated system based on a 2G Enterprises, Inc., three-axis superconducting magnetometer) in the Geophysics Laboratory of Ludwig-Maximilians-Universität (Munich). Thermal demagnetizations were carried out by an ASC furnace and alternating fields (AF) demagnetizations were done with a tumbler LD-A (AGICO Inc) alternating field demagnetizer. AGICO "Remasoft" software was used to analyze the magnetic behaviors of the samples and determine the characteristic remanent magnetizations (ChRM).

The ChRMs were determined , as described in Ruiz González et al. (2020), only in their geographic coordinates due to the lack of paleohorizontal evidence. Characteristic remanence directions (ChRM) with less than 15° of Maximum Angular Deviation (MAD) calculated using at least 3 demagnetization steps were exclusively accepted for the analysis (Kirschvink 1980). Samples with less than 20% of the NRM intensity after steps of 20 mT or 300 °C of demagnetization were discarded, considering that low coercivities (Hc) or low un-blocking temperatures could belong to spurious magnetic components. The paleomagnetic analysis was performed using the ChRMs of the samples without averaging them per site, according to Deenen et al. (2011), and each pluton was considered as belonging to the same tectonic block (Fig. 1C). A cut-off angle of 40° was applied to the ChRM to filter transitional and spurious data (Wilson et al., 1972). In order to validate these results, a reversal test was carried out with the ChRM directions inside the cut off angle.

196 To discuss the tectonic implications of the paleomagnetic results and detect possible
197 spatial variations in the amount of tectonic rotation and flattening values with respect to stable
198 South America for each pluton, we used Demarest (1983). The references paleopoles for
199 South America for 210 Ma (Cobquecura Pluton) and 220 Ma (Constitución Granite and
200 Hualpén Stock) were taken from Torsvik et al. (2012). The mean directions for each locality
201 and the tectonic rotations and inclination errors are given in Tables 1-4.

202 Nine sites were sampled in the granite (COS3-COS12, 50 cores) and one (COS13, 5
203 cores) in the host rock (Fig. 2a). Sampling covered mainly the western sector of the pluton
204 with a distance between adjacent sites generally around hundreds of meters (660m) up to 3
205 km. The Cobquecura Pluton was sampled at 4 localities (COB1 to COB4) at the northern part
206 of the pluton and one (COB5) at the southern part near to Santa Rita (30 cores in total) (Fig.
207 2c). Also, six sites were drilled in Hualpén stock located ~79 km to the south near to
208 Concepción city (HUA-1 to HUA-6; Fig. 2f). A total of 27 independently oriented cores were
209 obtained.

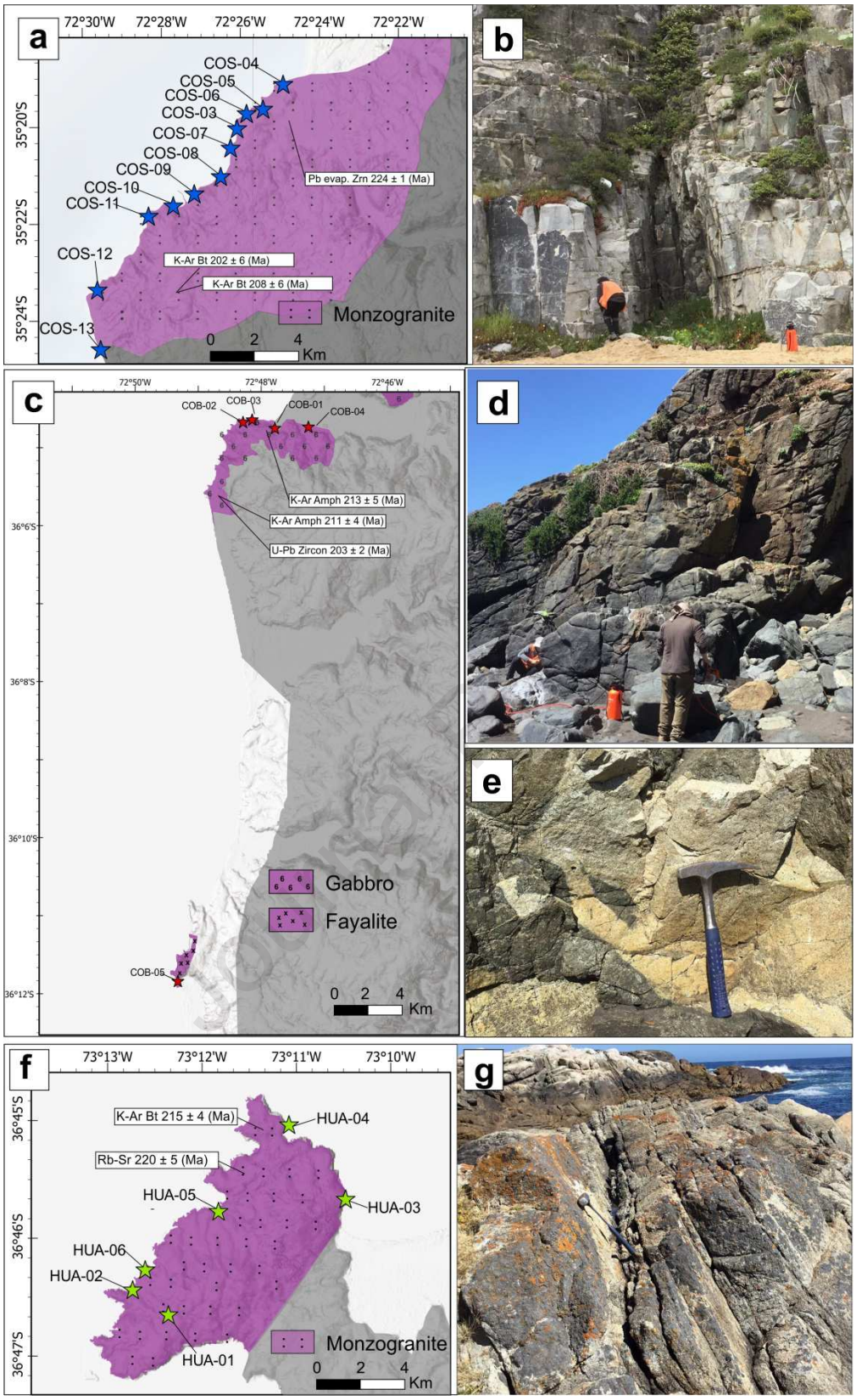

Figure 2: (a) Geological map of Constitución Granite. Ages from Willner et al. (2005) and Gana and Hervé (1983). (b) Outcrop view. (c) Geological map of Cobquecura Pluton. Radiometric ages from Vásquez et al. 2005 and 2011. (d) Outcrop view. (e) Felsic intrusion in gabbro. (f) Geological map of Hualpén Stock. Isotopic ages from Lucassen et al. (2004) and Hervé et al 1988. (g) Outcrop view with clearly developed subparallel joints. Blue, red and green stars show sampling locations in each studied unit.

4. Characteristic directions

In this section we analyse the paleomagnetic data obtained from the Constitución, Cobquecura and Hualpén plutons. In spite of the fact that in the three areas a characteristic remanence direction could be obtained of normal and reversed polarity and all correspond to Upper Triassic rocks, each pluton will be analyzed separately.

4.1. Constitución Granite

Characteristic remanence directions were obtained from most of the samples of the monzogranite (see Table 1). On the other hand, four of the five samples obtained from the host rock presented an erratic behavior during demagnetization procedures (Fig. 3f). The unique component obtained (sample COS13-3, see Table 1) shows an anomalous direction and was discarded for tectonic analysis.

For samples from the Constitución Granite both demagnetizing methods were efficient in isolating a stable univectorial normal or reverse polarity remanent magnetization (Fig. 3). The ChRM was recovered by thermal demagnetization in the temperature range 450-530ºC, or the range 10-60 mT under AF cleaning (Fig. 3). The characteristic component was determined with MAD under 10° in most cases (see Table 1). Since both polarities were recorded, the McFadden and McElhinny (1990) reversal test was performed. An indeterminate result was obtained with a $\gamma_{observed}$ =12.5° and a $\gamma_{critical}$ =28.1°.

The mean direction for the Constitución Granite obtained after ruling out eight ChRM considered anomalous differs from the expected Late Triassic paleomagnetic field suggesting a clockwise tectonic rotation of 13.5±11.5° (Fig. 3 II, see Table 4).

Table 1: Paleomagnetic results in geographic coordinates for the Constitución Granite.

Sample	Lat.	Long.	Lithology	Dec	Inc	MAD
			Constitución Pluton (~210 Ma)			
COS-03-1	-35.333	-72.435	Monzogranite	56.4	-53.8	7.5
COS-03-2	-35.333	-72.435	Monzogranite	----	----	----
COS-03-3	-35.333	-72.435	Monzogranite	----	----	----
COS-03-4	-35.333	-72.435	Monzogranite	----	----	----
COS-03-5	-35.333	-72.435	Monzogranite	----	----	----
COS-04-1	-35.318	-72.415	Monzogranite	11.	-41.2	9.1
COS-04-2	-35.318	-72.415	Monzogranite	352.3	-19.3	9.4
COS-04-3	-35.318	-72.415	Monzogranite	----	----	----

COS-04-4	-35.318	-72.415	Monzogranite	12.6	-34.7	9.8
COS-04-5	-35.318	-72.415	Monzogranite	307.2	-27.0	8.5
COS-05-1	-35.326	-72.424	Monzogranite	19.1	-21.5	8.1
COS-05-2	-35.326	-72.424	Monzogranite	274.2	-67.5	4.8
COS-05-3	-35.326	-72.424	Monzogranite	----	----	----
COS-05-4	-35.326	-72.424	Monzogranite	34.1	-49.6	3.5
COS-05-5	-35.326	-72.424	Monzogranite	8.4	-50.7	9.4
COS-06-1	-35.328	-72.431	Monzogranite	241.9	42.7	10.7
COS-06-2	-35.328	-72.431	Monzogranite	41.0	-41.0	9.6
COS-06-3	-35.328	-72.431	Monzogranite	19.5	-71.3	8.
COS-06-4	-35.328	-72.431	Monzogranite	12.3	23.7	9.5
COS-06-5	-35.328	-72.431	Monzogranite	16.2	-47.4	14.2
COS-07-1	-35.340	-72.437	Monzogranite	352.2	-37.0	7.4
COS-07-2	-35.340	-72.437	Monzogranite	----	----	----
COS-07-3	-35.340	-72.437	Monzogranite	----	----	----
COS-07-4	-35.340	-72.437	Monzogranite	353.3	-21.5	4.8
COS-07-5	-35.340	-72.437	Monzogranite	----	----	----
COS-08-1	-35.350	-72.441	Monzogranite	346.0	-56.7	8.3
COS-08-2	-35.350	-72.441	Monzogranite	47.3	-12.5	3.9
COS-08-3	-35.350	-72.441	Monzogranite	293.8	-7.2	8.8
COS-08-4	-35.350	-72.441	Monzogranite	25.1	-51.2	9.9
COS-08-5	-35.350	-72.441	Monzogranite	9.9	-65.0	8.1
COS-09-1	-35.356	-72.453	Monzogranite	24.3	-57.2	10.
COS-09-2	-35.356	-72.453	Monzogranite	22.6	-49.3	6.8
COS-09-3	-35.356	-72.453	Monzogranite	19.0	-61.3	9.
COS-09-4	-35.356	-72.453	Monzogranite	11.3	-71.4	10.3
COS-09-5	-35.356	-72.453	Monzogranite	13.6	-66.4	8.3
COS-10-1	-35.360	-72.462	Monzogranite	26.2	-65.3	9.8
COS-10-2	-35.360	-72.462	Monzogranite	27.1	-67.8	6.7
COS-10-3	-35.360	-72.462	Monzogranite	134.1	-79.9	9.4
COS-10-4	-35.360	-72.462	Monzogranite	45.6	-64.4	8.8
COS-10-5	-35.360	-72.462	Monzogranite	124.5	-69.9	9.5
COS-11-1	-35.363	-72.472	Monzogranite	60.8	-65.0	9.6
COS-11-2	-35.363	-72.472	Monzogranite	317.3	-45.7	7.4
COS-11-3	-35.363	-72.472	Monzogranite	153.7	47.5	4.1
COS-11-4	-35.363	-72.472	Monzogranite	122.5	-50.1	14.4
COS-11-5	-35.363	-72.472	Monzogranite	81.3	-56.7	3.9
COS-12-1	-35.389	-72.494	Monzogranite	14.0	-65.4	7.4
COS-12-2	-35.389	-72.494	Monzogranite	85.5	-71.0	7.8
COS-12-3	-35.389	-72.494	Monzogranite	31.1	-77.8	9.7
COS-12-4	-35.389	-72.494	Monzogranite	19.2	-43.3	8.2
COS-12-5	-35.389	-72.494	Monzogranite	64.9	-53.1	6.9
COS-13-1	-35.409	-72.492	Milonite	----	----	----
COS-13-2	-35.409	-72.492	Milonite	----	----	----
COS-13-3	-35.409	-72.492	Milonite	67.6	41.20	5.6
COS-13-4	-35.409	-72.492	Milonite	----	----	----

COS-13-5	-35.409	-72.492	Milonite	----	----	----
Mean		**N/n**	**Dec**	**Inc**	**α95**	**k**
COS		**35/55**	**15.4**	**-58.2**	**7.2**	**12**

Lat., Long.: site location (to the nearest half a minute). (n/N): number of samples involved in statistics/ total number of samples. Decl., Incl.: declination and inclination of paleomagnetic vector in geographical coordinates. α95: cone of 95% confidence level around mean direction (Fisher, 1953). k: precision parameter (Fisher, 1953). Sites not considered for mean calculation are highlighted in gray. Samples with (---) indicates that ChRM could not be obtained.

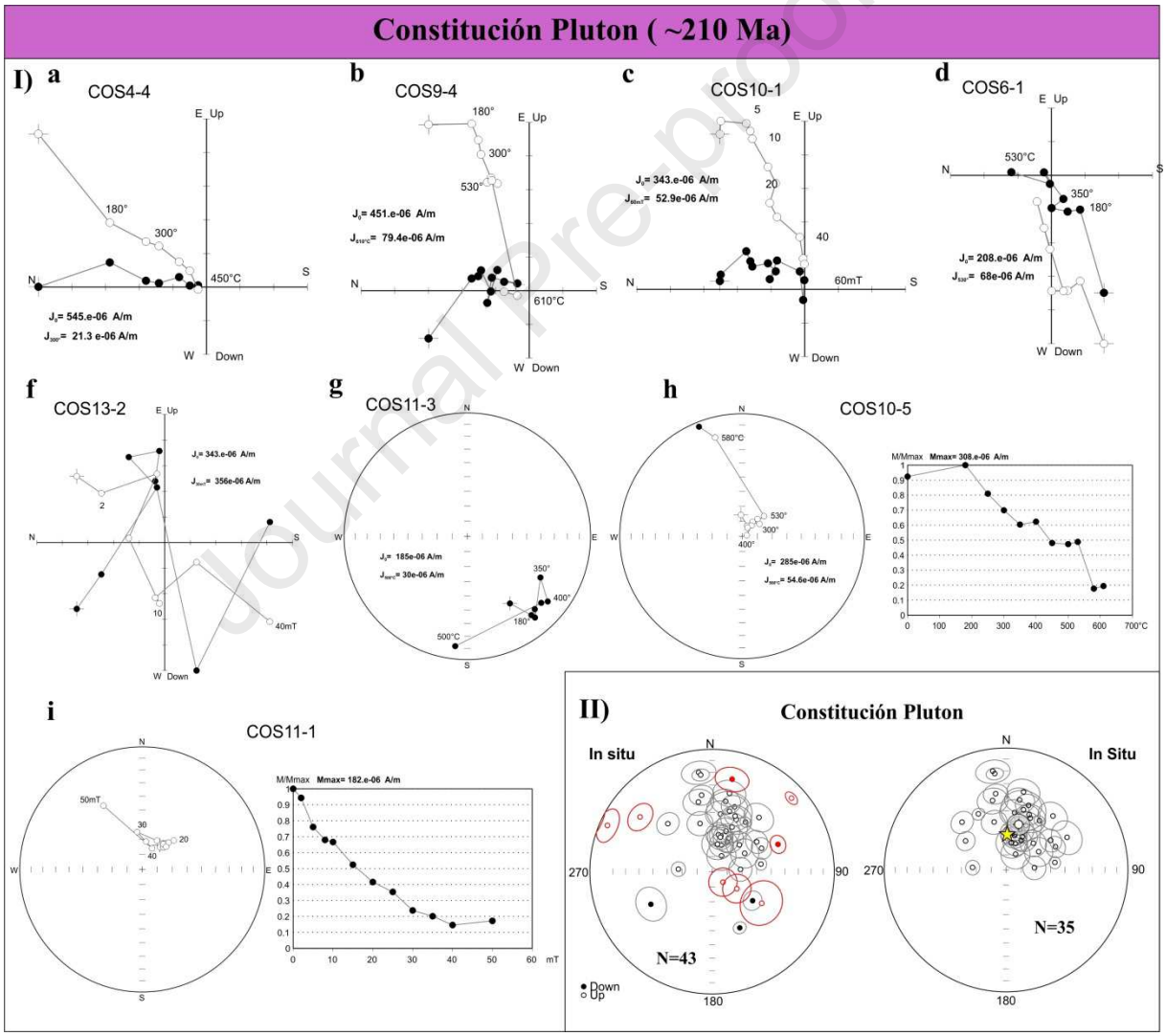

Figure 3:(I) Paleomagnetic behavior observed for samples from the Constitución Granite (a-e and g-i) and the host rock (f). The open (full) symbols in the Zijderveld diagram correspond to the projection in the vertical (horizontal) plane; in the stereonet open (full) symbols indicate up- wards (downwards) inclination. (II) To the left directions of the characteristic remanence of the specimens of Constitución Granite, samples discarded are showing in red; at right mean direction carried to a single polarity. Open (filled) symbols correspond to projection onto the upper (lower) hemisphere. The yellow star corresponds to the references direction.

247 4.2. Cobquecura Pluton

248 Samples from the pluton exhibited stable magnetic behaviors that allowed us to define
249 ChRM (see Table 2). These were mostly determined with MAD < 11°. Both demagnetization
250 methods were efficient in discriminating the magnetic components. In most cases, a unique
251 ChRM was isolated at temperatures/ maximum alternating fields ranges of 180-580°C or 10-
252 60mT (Fig.4I a-b and d-f). Sometimes thermal demagnetization showed an abrupt decay of
253 the remanence towards the origin of coordinates above 500 °C (Fig. 4I-e and f). Samples from
254 COB2 record two components, one of lower temperature (180-350°C) and other between 400-
255 580°C (Fig.4I-c). The lower temperature component shows scattered directions and was
256 discarded from further analysis (see Table 2). These differences in the demagnetization
257 behaviors between different sites reflect the widely variable textural and compositional
258 lithology of the pluton.

259 Remanences of this intrusive body record both polarities of the paleomagnetic field
260 (Fig.4II), although positive inclinations predominate. The reversal test of McFadden and
261 McElhinny (1990) was performed with an indeterminate result: $\gamma_{observed}$ =19° and a $\gamma_{critical}$
262 =21.3°. The mean direction obtained for the Cobquecura Pluton differs from the expected
263 direction (see star in Fig. 4II and Table 4) suggesting a 41.3±15°clockwise rotation (Fig. 4II).

264

265 **Table 2: Paleomagnetic results from Cobquecura Pluton**

Sample	Lat.	Long.	Lithology	Dec	Inc	MAD
Cobquecura Pluton (~209 Ma)						
COB1-1	-36.079	-72.796	Gabbro	26.6	-12.6	8.6
COB1-2	-36.079	-72.796	Gabbro	----	----	----
COB1-3C	-36.079	-72.796	Gabbro	9.3	-56.3	10.3
COB1-4	-36.079	-72.796	Gabbro	87.3	-66.6	5.8
COB1-5	-36.079	-72.796	Gabbro	83.6	-67.8	9.4
COB1-6A	-36.079	-72.796	Gabbro	48.6	-73.1	8.4
COB2-1^{l}	-36.077	-72.802	Gabbro	139.6	1.1	2.6
COB2-1^{h}	-36.077	-72.802	Gabbro	47.8	-56.1	1.8
COB2-2C^{l}	-36.077	-72.802	Gabbro	74.2	-3.7	8.6
COB2-2C^{l}	-36.077	-72.802	Gabbro	337.4	4.4	4
COB2-2C^{h}	-36.077	-72.802	Gabbro	333.1	-40.2	9.4
2COB-2	-36.077	-72.802	Gabbro	222.1	-34	10.8
COB2-3^{h}	-36.077	-72.802	Gabbro	49.9	-62.9	5.3
COB2-3^{l}	-36.077	-72.802	Gabbro	96.1	-37	4.2
COB2-4	-36.077	-72.802	Gabbro	31.5	-11.1	3.2

COB2-5	-36.077	-72.802	Gabbro	15.1	7.4	4.9
COB2-6	-36.077	-72.802	Gabbro	18.8	-64.2	6.2
COB3-1	-36.078	-72.805	Gabbro	122.1	51.5	8.4
COB3-2	-36.078	-72.805	Gabbro	----	----	----
COB3-3	-36.078	-72.805	Gabbro	27.7	-43.8	10.3
COB3-4	-36.078	-72.805	Gabbro	267.7	79.6	8.9
COB3-5	-36.078	-72.805	Gabbro	153.8	78.3	5.1
COB3-6B	-36.078	-72.805	Gabbro	318.8	9	8.7
COB4-1	-36.079	-72.788	Fayalite	----	----	----
COB4-2	-36.079	-72.788	Fayalite	38.3	-61.1	5.2
COB4-2A	-36.079	-72.788	Fayalite	38	-58.8	9.8
COB4-3	-36.079	-72.788	Fayalite	40.6	-72.4	3.1
COB4-4	-36.079	-72.788	Fayalite	168.3	-73.8	13
COB4-5	-36.079	-72.788	Fayalite	45.6	-60.3	8.2
COB5-1B	-36.197	-72.822	Gabbro	272.9	66.4	9.3
COB5-2	-36.197	-72.822	Gabbro	271.5	69	6.3
COB5-3	-36.197	-72.822	Gabbro	----	----	----
COB5-4	-36.197	-72.822	Gabbro	280	64.2	3.2
COB5-5	-36.197	-72.822	Gabbro	275.6	72.7	2.5
Mean		**N/n**	**Dec**	**Inc**	**α95**	**k**
COB		**22/29**	**232.1**	**68.4**	**6.7**	**28**

Lat., Long.: site location (to the nearest half a minute). (n/N): number of samples involved in statistics/ total number of samples. Decl., Incl.: declination and inclination of paleomagnetic vector in geographical coordinates. α95: cone of 95% confidence level around mean direction (Fisher, 1953). k: precision parameter (Fisher, 1953). Sites not considered for mean calculation are highlighted in gray. ^{h}: High temperature component. ^{l}: Low temperature component. Samples with (---) indicates that ChRM could not be obtained.

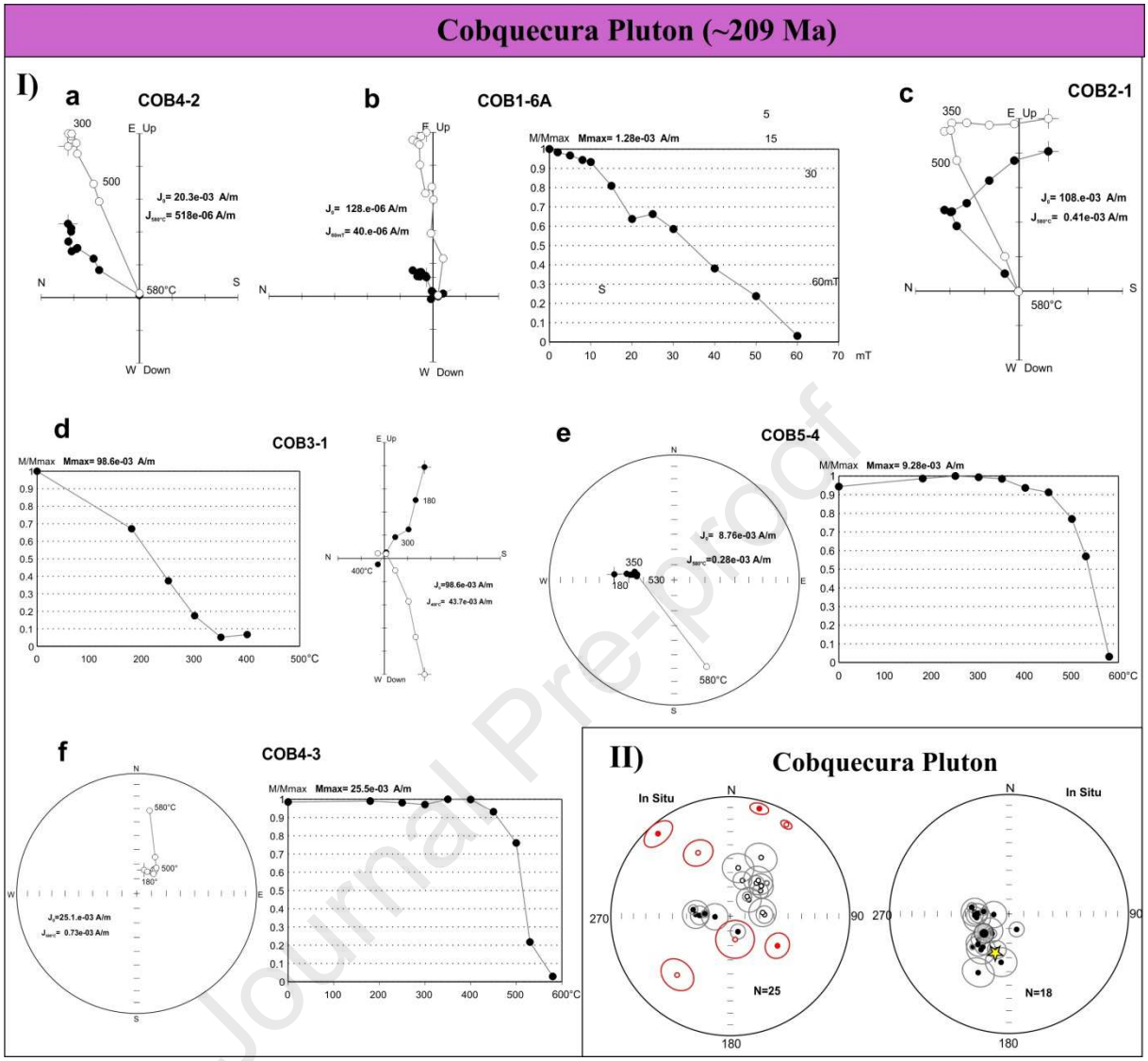

Figure 4: (I) Paleomagnetic behaviour observed in Cobquecura Pluton. See text for explanation. The open (full) symbols in the Zijderveld diagram correspond to the projection in the vertical (horizontal) plane; in the stereonet open (full) symbols indicate upwards (downwards) inclination.. (II) Directions of the ChRM showing in red are not involved in the calculation of the mean. To the right mean direction carried to reversed polarity, the star corresponds to the expected direction.

4.3. Hualpén Stock

Characteristic remanence directions of both polarities were obtained from most of the samples of the Hualpén Stock (see Table 3, Fig.5). In most cases, a unique component decaying towards the origin could be isolated between 180-580°C or 10-60mT (Fig.5I). Sometimes an abrupt decay during thermal demagnetization was observed above 500 °C (Fig. 5I-b and e) suggesting that titano-magnetite is the main mineral carrying the remanence. A few samples from the stock record two components: one of lower temperature (180-300°C) and another between 350-580°C (Fig.5I-f). In contrast with the Cobquecura Pluton, most of

the remanence of lower temperature observed in the Hualpén Stock record a direction similar to the samples with a unique component (see Table 3).

Since both polarities were recorded, the reversal test of McFadden and McElhinny (1990) was performed. An indeterminate result was obtained with an $\gamma_{observed}$ =2.6° and a $\gamma_{critical}$ =24.1°. The mean direction obtained from the stock, after applying a cut-off angle of 45° to filter transitional and spurious data, differs from the expected paleomagnetic field for the Late Triassic suggesting that the stock is 16±16.3° counter-clockwise rotated (Fig. 5II and Table 4).

Table 3: Characteristic remanence directions from Hualpén Stock.

Sample	Lat.	Long.	Lithology	Dec	Inc	MAD
Hualpén Stock (~217 Ma)						
HUA1-1	-36.777	-73.206	Monzogranite	348.9	-80.1	7.6
HUA1-2	-36.777	-73.206	Monzogranite	3.8	25.6	7.8
HUA1-3	-36.777	-73.206	Monzogranite	285.2	-86.5	7.9
HUA2-1B	-36.774	-73.212	Monzogranite	319.2	-57.3	6.3
HUA2-2	-36.774	-73.212	Monzogranite	32.3	-62.1	7.5
HUA2-3^{l}	-36.774	-73.212	Monzogranite	319.3	-60.3	9
HUA2-3^{h}	-36.774	-73.212	Monzogranite	176.7	64.6	10
HUA2-4^{h}	-36.774	-73.212	Monzogranite	198.5	64.8	6.7
HUA2-4^{l}	-36.774	-73.212	Monzogranite	352.4	-51.3	3
HUA2-5	-36.774	-73.212	Monzogranite	180.7	33.6	8.5
HUA3-1^{l}	-36.761	-73.175	Monzogranite	264.4	3.2	0.4
HUA3-1^{h}	-36.761	-73.175	Monzogranite	41.9	57.6	6
HUA3-2	-36.761	-73.175	Monzogranite	254.6	40	9.4
HUA3-3	-36.761	-73.175	Monzogranite	278.2	73.8	5.4
HUA3-4	-36.761	-73.175	Monzogranite	175.5	-21	13.9
HUA3-5	-36.761	-73.175	Monzogranite	335.7	-28.2	11.9
HUA3-6	-36.761	-73.175	Monzogranite	326.9	39	6.8
HUA4-1	-36.751	-73.185	Monzogranite	228.4	42.6	2.2
HUA4-2	-36.751	-73.185	Monzogranite	----	----	----
HUA4-3	-36.751	-73.185	Monzogranite	257.8	28.3	3
HUA4-4	-36.751	-73.185	Monzogranite	111.5	57.5	3.3
HUA4-5	-36.751	-73.185	Monzogranite	19.7	36.6	12.4
HUA5-1	-36.763	-73.197	Monzogranite	43.4	-75.4	9
HUA5-2	-36.763	-73.197	Monzogranite	3.4	-55.3	8
HUA5-3	-36.763	-73.197	Monzogranite	331.8	-58.5	9.2
HUA5-4^{l}	-36.763	-73.197	Monzogranite	341.8	-63.2	11.2
HUA5-4^{h}	-36.763	-73.197	Monzogranite	227.5	19.2	8.6
HUA6-1	-36.771	-73.210	Monzogranite	7.4	-48	6.9
HUA6-2^{l}	-36.771	-73.210	Monzogranite	324.1	-24.6	6.3

HUA6-2[h]	-36.771	-73.210	Monzogranite	63.8	21.6	12.8
HUA6-4	-36.771	-73.210	Monzogranite	291.1	51.1	9
HUA6-5	-36.771	-73.210	Monzogranite	254.6	68.1	14.7
Mean		**N/n**	**Dec**	**Inc**	**α95**	**k**
HUA		**17/32**	**165.6**	**60**	**9.9**	**14**

Same as Table 2

290

291

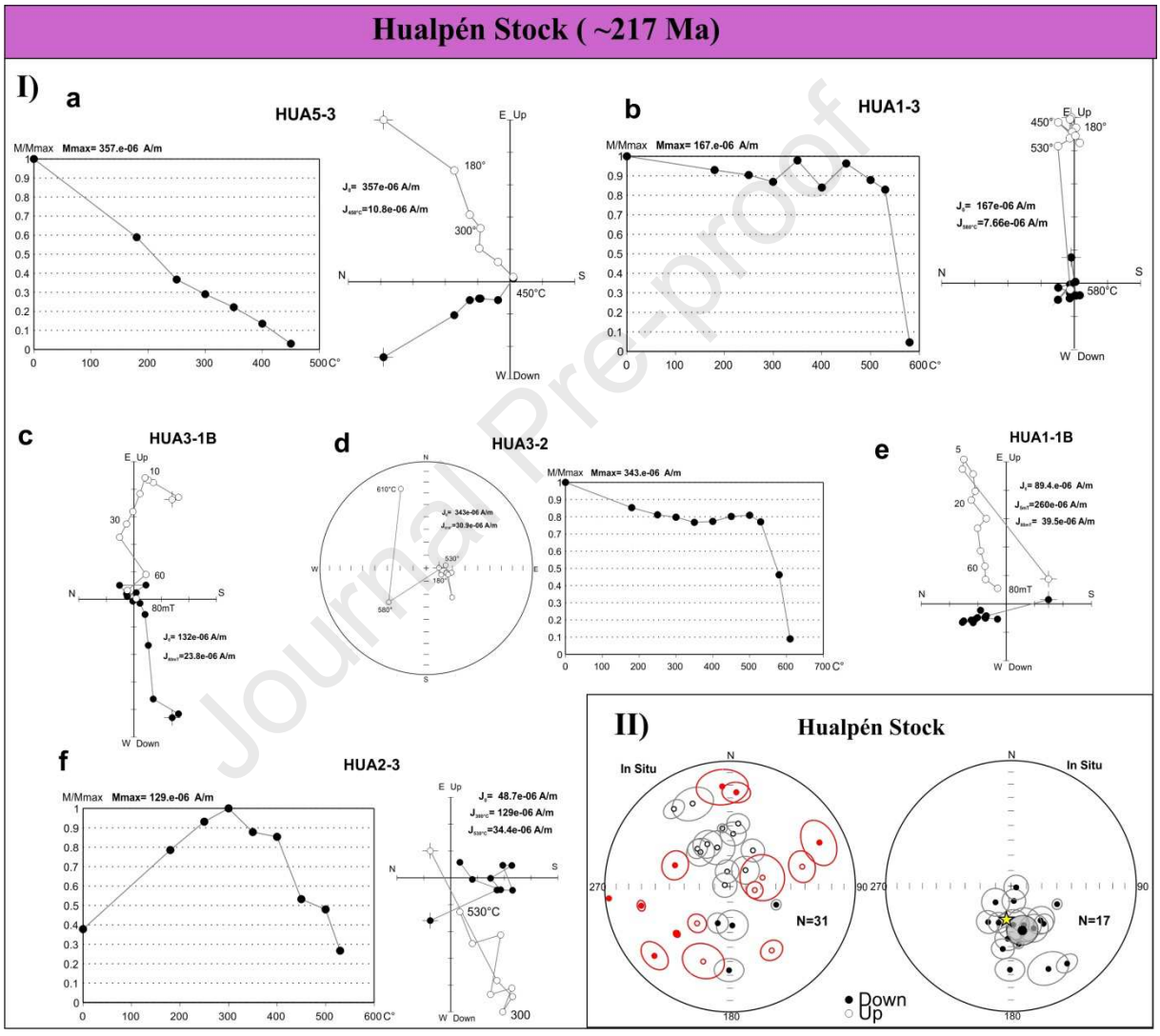

292

293 **Figure 5: (I) Paleomagnetic behavir observed in Hualpén Stock. (a-e) AF or thermal demagnetization plots for**
294 **representative samples with a unique component. (f) Sample showing two components. See Fig.1 for references. (II)**
295 **Directions of the ChRM showing in red the direction discarded in the calculation of the mean (left). To the right mean**
296 **direction transposed to reverse polarity, the star corresponds to the expected direction.**

297

298 ## 5. Tectonic rotations

For each locality, tectonic rotations and inclination anomalies were calculated according to Demarest et al. (1983) using the reference poles for 210 Ma and 220 Ma from Torsvik et al (2012) transported to South American coordinates through the translations proposed in that work (see Table 4).

Table 4: Tectonic rotations

Locality	Lat.	Long	age ref.	Dec.obs.	Inc.obs	α95	Dec.exp	Inc.exp	α95	R± ΔR	I± ΔI
Constitución Granite	-35.3	-72.4	220	15.4	-58.2	7.2	1.9	-68.1	1.5	13.5±11.5	9.9±5.8
Cobquecura Pluton	-36.1	-72.8	210	232.1	68.4	6.7	190.8	66	1.5	41.3±15	-2.4±5.5
Hualpén Stock	-36.7	-73.2	220	165.6	60	9.9	181.6	68.1	1.5	-16.0±16.4	9.1±8.0

Age: estimated age of the magnetization and of the reference from Torsvik et al. (2012) used to calculate the rotation; Lat, Long: Latitude, longitude, position of the locali- ties used in the calculation of the tectonic parameters; Dobs, Iobs: observed paleomagnetic declination and inclination; a95: semi-angle of confidence; Dexp, Iexp: are the expected declination and inclination from expected pole; R(°),ΔR, I(°), ΔI: rotation and inclination and their associated errors (Demarest, 1983).

The data obtained indicate an increase in the magnitude of a clockwise tectonic rotation between the Constitución Granite and the Cobquecura Pluton from ~13° up to 41°. This is consistent with previous paleomagnetic data (Beck et al. 1986, 1990; Charrier et al. 1996; Goguitchaichvili et al. 2000; Parada et al. 2005; Astudillo et al. 2009; Arriagada et al. 2013) (see Fig. 6). On the other hand, the Hualpén Stock recorded minor counter-clockwise tectonic rotation to no tectonic rotation. The spatial variation in the magnitude and sense of rotations shows that the Chilean Andes region between 30º and 37ºS did not behave as a rigid block.

Previous paleomagnetic data show no significant systematic rotations in Chile between approximately 31° and 33 ° S (Dashwood and Taylor 2005; Peña et al. 2011; Arriagada et al. 2013;Fig. 6). To the south of this last segment, a new zone of clockwise tectonic rotations is observed between approximately 33° and 36° S (see Arriagada et al. 2013 and references therein). This last area is limited to the north by the Argentinian Precordillera, where one of the orogenic maximums in Neogene horizontal shortening is observed (Fig. 6b). Horizontal shortening decreases gradually between 33 ° and 36 ° S (Giambiagi et al. 2012). Dewey and Lamb (1992) interpreted that this decrease in the horizontal shortening would be responsible for a clockwise oroclinal rotation of the trench and volcanic arc between 34 ° and 39 °S, and the formation of the Maipo Orocline (Arriagada et al. 2009). This hypothesis is in agreement

with the previous paleomagnetic data (Beck et al. 1986, 1990; Charrier et al. 1996; Goguitchaichvili et al. 2000; Parada et al. 2005; Astudillo et al. 2009; Arriagada et al. 2013).

Japas and Re (2012) presented an alternative interpretation in which the Maipo Orocline would have been part of the Bolivian Orocline, later disconnected from northern Chile by a counter-clockwise rotation of the coastal segment between 30° and 33°S. These authors attributed this younger counter-clockwise rotation to the subduction of Juan Fernández ridge, so that the collision of the ridge would have almost entirely restored the deflection caused by the hourly rotation of the Bolivian Orocline to an orientation close to the pre-oroclinal.

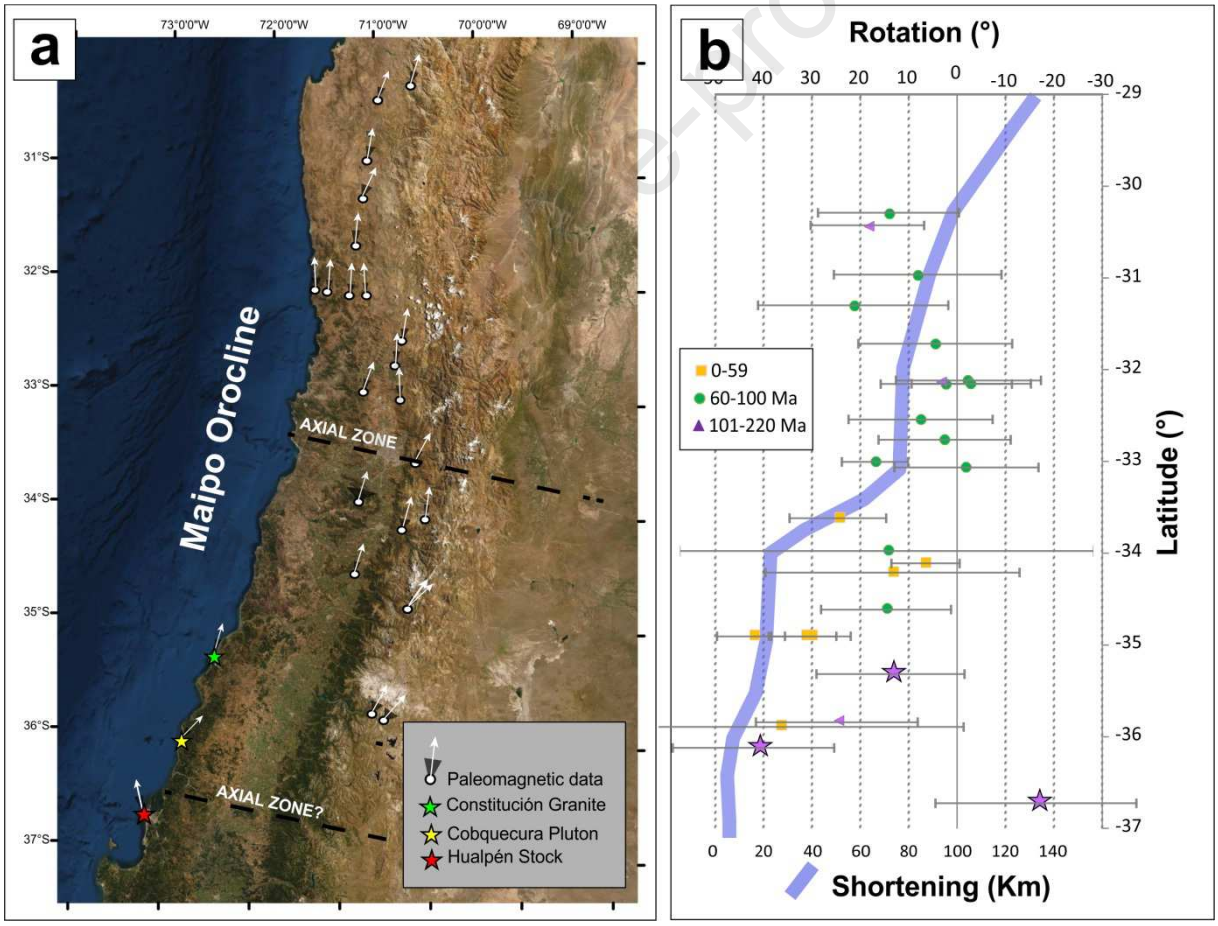

Figure 6: (a) Compilation of tectonic rotations (deviation of arrows from a NS direction) with errors between 30° and 37°S. (b) Paleomagnetic rotation colored by ages of magnetization plotted against latitude. Blue line corresponded to a maximum horizontal shortening according to Allmendinger et al. (1990); von Gosen (1992); Ramos et al. (1996, 2002); Giambiagi et al. (2012); Allmendinger and Judge (2014); Rojas Vera et al. (2014)**. Stars correspond to this study.**

The paleomagnetic rotations obtained in this work for the Constitución Granite and Cobquecura Pluton are similar to data reported by Arriagada et al. (2013) for a 10 Ma

intrusive rocks suggesting that all the area rotated as a single block during the Miocene (Fig. 6). Results obtained by Astudillo et al. (2009)) show that no rotations occurred since 5 Ma. The large tectonic rotation observed in Cobquecura Pluton exceeds the expected tectonic rotation due to horizontal shortening. This rotation can be explained as a consequence of a transfer zone to accommodate the change in style and distribution of deformation between Cobquecura Pluton and counter-clockwise to insignificant tectonic rotation obtained from Hualpén Stock. In that case, the Maipo and Arauco Oroclines limit is located to the north of the stock. However, more paleomagnetic and structural data is needed in order to corroborate this hypothesis.

6. Conclusion

Paleomagnetic data obtained from the Upper Triassic Constitución Granite and Cobquecura Pluton indicate an increase of clockwise tectonic rotations from north to south. The similar amounts of tectonic rotations recorded by Mesozoic and Miocene rocks suggest that no rotations occurred in the area during the Gondwana breakup. Considering the good correspondence between the balanced section analyses with the paleomagnetic data, we believe that the deflection in the trench heading and the tectonic rotations of this segment respond to differential shortening north of ~36°S. In contrast, the Hualpén granite (~217 Ma) registers minor to insignificant counter-clockwise rotations for the southern area. This change from north to south suggests that the boundary between the Maipo and Arauco oroclines is located to the north of the Hualpén granite.

Acknowledgment

This study was funded through the FONDECYT Iniciación grant 11160329 (Pablo Rossel) and the regular UNAB proyect DI-1278-16/R (Pablo Rossel). F. Carvajal is thanked for assistance in field work. Super IAPD software packages by Torsvik (NGU) and Remasoft program (AGICO SA) were used to analyse the data. Thanks to the two anonymous referees for provided careful and constructive reviews to our manuscript.

References

Aguirre L, Hervé F, Godoy E (1972) Distribution of metamorphic facies in Chile, an outline. Kristalinikum 9:7–19

Allmendinger RW, Figueroa D, Snyder D, et al (1990) Foreland shortening and crustal balancing in the Andes at 30°S latitude. Tectonics 4:789–809

Allmendinger RW, Judge PA (2014) The argentine precordillera: A foreland thrust belt proximal to the subducted plate. Geosphere 10:1203–1218. doi: 10.1130/GES01062.1

Arriagada C, Ferrando R, Córdova L, et al (2013) El Oroclino del Maipo: Un rasgo estructural de primer orden en la evolución geodinámica Mioceno a Reciente en los Andes de Chile central. Andean Geol 40:419–437. doi: 10.5027/andgeoV40n3-a02

Arriagada C, Mpodozis C, Yañez G, et al (2009) Rotaciones tectónicas en Chile central : El oroclino de Vallenar y el " megakink " del Maipo. In: XII Congreso Geologico Chileno. Santiago de Chile, pp 1–4

Astudillo N, Roperch P, Townley B, et al (2009) Magnetic polarity zonation within the El Teniente copper-molybdenum porphyry deposit, central Chile. Miner Depos 45:23–41. doi: 10.1007/s00126-009-0256-0

Bahlburg H, Hervé F (1997) Geodynamic evolution and tectonostratigraphic terranes of northwestern Geodynamic evolution and tectonostratigraphic terranes of northwestern Argentina and northern Chile. Geol Soc Am Bull 109:869–884. doi: 10.1130/0016-7606(1997)109<0869

Beck ME, Burmester RF, Garcia A, Rivano S (1990) Paleomagnetic Results From Cretaceous Rocks in the Llaiillay-San Felipe-Putaendo Region: implications for block rotations in the Andean Forearc. Rev Geol Chile 17:115–130

Beck ME, Drake RE, Butler RF (1986) Paleomagnetism of Cretaceous volcanic rocks from central Chile and implications for the tectonics of the Andes. Geology 14:132–136. doi: 10.1130/0091-7613(1986)14<132:POCVRF>2.0.CO;2

Beck ME, Garcia R. A, Burmester RF, et al (1991) Paleomagnetism and geochronology of late Paleozoic granitic rocks from the Lake District of southern Chile: implications for accretionary tectonics. Geology 19:332–335. doi: 10.1130/0091-7613(1991)019<0332:PAGOLP>2.3.CO;2

Berg K, Breitkreuz C (1983) Mesozoische Plutone in der Nordchilenischen Kustenkordillere: Petrouenese. Geochronologie, Geochemie und Geodynamik mantelbetonter magmatique. Geotektonische Forsch 66:107

Berg K, Breitkreuz C, Damm KW, et al (1983) The North-Chilean Coast Range - an example for the development of an active continental margin. Geol Rundschau 72:715–731. doi: 10.1007/BF01822090

Carey SW (1955) The orocline concept in geotectonics-Part I. Pap Proc R Soc Tasmania 89:255–288

Charrier R (1979) El Triásico en Chile y regiones adyacentes de Argentina: una reconstrucción paleogeográfica y paleoclimática. Communicaciones 26:1–37

Charrier R, Farías M, Maksaev V (2009) Evolución tectónica, paleogeográfica y metalogénica durante el cenozoico en los Andes de Chile Norte y Central e implicaciones para las regiones adyacentes de Bolivia y Argentina. Rev la Asoc Geol Argentina 65:5–35

Charrier R, Wyss AR, Flynn JJ, et al (1996) New evidence for Late Mesozoic-Early Cenozoic evolution of the Chilean Andes in the Upper Tinguiririca Valley (35°s), central Chile. J South Am Earth Sci 9:393–422. doi: 10.1016/s0895-9811(96)00035-1

Coira B, Davidson J, Mpodozis C, Ramos V (1982) Tectonic and magmatic evolution of the Andes of northern Argentina and Chile. Earth Sci Rev 18:303–332. doi: 10.1016/0012-8252(82)90042-3

Creixell C, Lucassen F, Franz G, et al (2002) Petrology of Hualpen stock : evidences of Late Triassic crustal epizonal plutonism at the Western margin of Gondwana (36°45 ' S – 73°10 ' W). In: V ISAG. Toulouse-France, pp 167–170

Creixell C, Parada MÁ, Roperch P, et al (2006) Syntectonic emplacement of the Middle Jurassic Concón Mafic Dike Swarm,

Coastal Range, central Chile (33° S). Tectonophysics 425:101–122. doi: 10.1016/j.tecto.2006.07.005

Dashwood B, Taylor GK (2005) Temporal and spatial constraints on multi-phase crustal rotaltion in the forearc of northern Chile. 6th Int Symp Andean Geodyn (ISAG 2005, Barcelona), Ext Abstr 202-205 202–205

Deenen MHL, Langereis CG, van Hinsbergen DJJ, Biggin AJ (2011) Geomagnetic secular variation and the statistics of palaeomagnetic directions. Geophys J Int 186:509–520. doi: 10.1111/j.1365-246X.2011.05050.x

Demarest Harold H. (1983) Error Analysis for the Determination of tectonic rotation from paleomagnetic data. J Geophys Res 88:4321–4328

Dewey JF, Lamb SH (1992) Active tectonics of the Andes. Tectonophysics 205:79–95. doi: 10.1016/0040-1951(92)90419-7

Farías M, Charrier R, Carretier S, et al (2008) Late Miocene high and rapid surface uplift and its erosional response in the Andes of central Chile (33° - 35°S). Tectonics 27:. doi: 10.1029/2006TC002046

Ferrando R, Roperch P, Morata D, et al (2014) A paleomagnetic and magnetic fabric study of the Illapel Plutonic Complex, Coastal Range, central Chile: Implications for emplacement mechanism and regional tectonic evolution during the mid-Cretaceous. J South Am Earth Sci 50:12–26. doi: 10.1016/J.JSAMES.2013.11.007

Fisher, R.A. (1953) Dispersion on a sphere. Proc. R. Soc. London Ser. A:217:295-305

Gana P, Hervé F (1983) Geología del basamento cristalino en la Cordillera de la Costa entre los ríos Mataquito y Maule, VII Región. Rev geológica Chile An Int J andean Geol 0:37–56. doi: 10.5027/ANDGEOV10N2-3-A03

Giambiagi L, Mescua J, Bechis F, et al (2012) Thrust belts of the southern Central Andes: Along-strike variations in shortening, topography, crustal geometry, and denudation. Bull Geol Soc Am 124:1339–1351. doi: 10.1130/B30609.1

Glodny J, Echtler H, Figueroa O, et al (2006) Long-Term Geological Evolution and Mass-Flow Balance of the South-Central Andes. In: The Andes. Springer Berlin Heidelberg, pp 401–428

Glodny J, Lohrmann J, Echtler H, et al (2005) Internal dynamics of a paleoaccretionary wedge: Insights from combined isotope tectonochronology and sandbox modelling of the South-Central Chilean forearc. Earth Planet Sci Lett 231:23–39. doi: 10.1016/j.epsl.2004.12.014

Goguitchaichvili A, Chauvin A, Roperch P, et al (2000) Palaeomagnetism of the Miocene Farellones formation (Chile). Geophys J Int 140:357–373. doi: 10.1046/j.1365-246x.2000.00022.x

Hervé F, Munizaga F, Parada MA, et al (1988) Granitoids of the Coast Range of central Chile: Geochronology and geologic setting. J South Am Earth Sci 1:185–194. doi: 10.1016/0895-9811(88)90036-3

Isacks BL (1988) Uplift of the Central Andean Plateau and bending of the Bolivian orocline. J Geophys Res 93:3211–3231. doi: 10.1029/JB093iB04p03211

Japas MS, Re GH (2012) Neogene Tectonic Block Rotations and Margin Curvature At the Pampean Flat Slab Segment (28^{o}-33^{o} Sl , Argentina). Geoacta 37:1–4

Kirschvink JL (1980) The least-squares line and plane and the analysis of palaeomagnetic data. Geophys J Int 62:699–718. doi: 10.1111/j.1365-246X.1980.tb02601.x

Lucassen F, Trumbull R, Franz G, et al (2004) Distinguishing crustal recycling and juvenile additions at active continental margins: The Paleozoic to recent compositional evolution of the Chilean Pacific margin (36-41°S). J South Am Earth Sci 17:103–119. doi: 10.1016/j.jsames.2004.04.002

Martin MW, Kato TT, Rodriguez C, et al (1999) Evolution of the late Paleozoic accretionary complex and overlying forearc-magmatic arc, south central Chile (38°-41°S): Constraints for the tectonic setting along the southwestern margin of Gondwana. Tectonics 18:582–605. doi: 10.1029/1999TC900021

McFadden PL, McElhinny MW (1990) Classification of the reversal test in palaeomagnetism. Geophys J Int 103:725–729. doi: 10.1111/j.1365-246X.1990.tb05683.x

Melnick D, Bookhagen B, Strecker MR, Echtler HP (2009) Segmentation of megathrust rupture zones from fore-arc deformation patterns over hundreds to millions of years, Arauco peninsula, Chile. J Geophys Res 114:1407. doi: 10.1029/2008JB005788

Mpodozis C, Kay S (1990) Provincias magmaticas acidas y evolucion tectonica de Gondwana : Andes Chilenos (28-31°S). Rev geol Chile 17:153–180. doi: 10.5027/andgeoV17n2-a03

Mpodozis C, Ramos VA (1989) The Andes of Chile and Argentina, in: Geology of the Andes and its Relation to Hydrocarbon and Mineral Resources. 11:59–90

Parada MA, Féraud G, Fuentes F, et al (2005) Ages and cooling history of the Early Cretaceous Caleu pluton: Testimony of a switch from a rifted to a compressional continental margin in central Chile. J Geol Soc London 162:273–287. doi: 10.1144/0016-764903-173

Peña M, Arriagada C, Martinez F, Creixell C (2011) Oroclino de Vallenar : Un estudio Geológico y Paleomagnético . In: Latinmag letters. Tandil-Argentina, pp 1–6

Ramos VA, Cegarra M, Cristallini E (1996) Cenozoic tectonics of the High Andes of west-central Argentina (30–36°S latitude). Tectonophysics 259:185–200. doi: 10.1016/0040-1951(95)00064-X

Ramos VA, Cristallini EO, Pérez DJ (2002) The Pampean flat-slab of the Central Andes. J South Am Earth Sci 15:59–78. doi: 10.1016/S0895-9811(02)00006-8

Rehak K, Strecker MR, Echtler HP (2008) Morphotectonic segmentation of an active forearc, 37°-41°S, Chile. Geomorphology 94:98–116. doi: 10.1016/j.geomorph.2007.05.002

Richter PP, Ring U, Willner AP, Leiss B (2007) Structural contacts in subduction complexes and their tectonic significance: The Late Palaeozoic coastal accretionary wedge of central Chile. J Geol Soc London 164:203–214. doi: 10.1144/0016-76492005-181

Rojas Vera EA, Folguera A, Zamora Valcarce G, et al (2014) Structure and development of the Andean system between 36° and 39°S. J Geodyn 73:34–52. doi: 10.1016/j.jog.2013.09.001

Ruiz González V, Puigdomenech CG, Zaffarana CB, et al (2020) Paleomagnetic evidence of the brittle deformation of the Central Patagonian Batholith at Gastre area (Chubut Province, Argentina). J South Am Earth Sci 98:102442. doi: 10.1016/j.jsames.2019.102442

Suarez M, Bell CM (1992) Triassic rift-related sedimentary basins in northern Chile (24°-29°S). J South Am Earth Sci 6:109–121. doi: 10.1016/0895-9811(92)90001-F

Torsvik TH, Van der Voo R, Preeden U, et al (2012) Phanerozoic polar wander, palaeogeography and dynamics. Earth-Science Rev 114:325–368. doi: 10.1016/j.earscirev.2012.06.007

Uliana MA, Biddle KT (1988) Mesozoic-Cenozoic Paleogeographic and geodynamic evolution of Southern South America. Rev Bras Geociências 18:172–190. doi: 10.25249/0375-7536.1988182172190

Vásquez P, Franz G (2008) The Triassic Cobquecura Pluton (Central Chile): An example of a fayalite-bearing A-type intrusive massif at a continental margin. Tectonophysics 459:66–84. doi: 10.1016/j.tecto.2007.11.067

Vásquez P, Franz G, Wemmer K (2005) Fe-rich silicates in the Cobquecura pluton: an indicator ofA-type granitoids in the Triassic magmatism of south-central Chile. In: 6th International Symposium on Andean Geodynamics. Barcelona, Spain, pp 773–775

Vásquez P, Glodny J, Franz G, et al (2009) Origin of fayalite granitoids: New insights from the Cobquecura Pluton, Chile, and its metapelitic xenoliths. Lithos 110:181–198. doi: 10.1016/j.lithos.2009.01.001

Vásquez P, Glodny J, Franz G, et al (2011) Early Mesozoic plutonism of the Cordillera de la Costa (34°-37°s), Chile: Constraints on the onset of the Andean Orogeny. J Geol 119:159–184. doi: 10.1086/658296

Von Gosen W (1992) Structural evolution of the Argentine Precordillera: the Río San Juan section. J Struct Geol 14:643–667. doi: 10.1017/CBO9781107415324.004

Willner AP, Thomson SN, Kröner A, et al (2005) Time markers for the evolution and exhumation history of a Late Palaeozoic paired metamorphic belt in North-Central Chile (34°-35°30′S). J Petrol 46:1835–1858. doi: 10.1093/petrology/egi036

Wilson R.L., Dagley P., McCormack A.G., et al (1972). Palaeomagnetic evidence about the source of the geomagnetic field. Geophysical Journal of the Royal Astronomical Society, 28 (1972), pp. 213-224.

Yáñez G, Cembrano J, Pardo M, et al (2002) The Challenger-Juan Fernández-Maipo major tectonic transition of the Nazca-Andean subduction system at 33-34°S: geodynamic evidence and implications. J South Am Earth Sci 15:23–38. doi: 10.1111/jace.13350

Paleomagnetic data from Upper Triassic rocks in southern Chile is presented.

Vertical-axis rotations related to Maipo Orocline formation are recorded.

Counter-clockwise rotation observed in Hualpén Stock suggests that the boundary between the Maipo and Arauco oroclines is located to the north.

Declaration of interests

☒ The authors declare that they have no known competing financial interests or personal relationships that could have appeared to influence the work reported in this paper.

☐The authors declare the following financial interests/personal relationships which may be considered as potential competing interests: